

This article was downloaded by:

On: 26 January 2011

Access details: *Access Details: Free Access*

Publisher *Taylor & Francis*

Informa Ltd Registered in England and Wales Registered Number: 1072954 Registered office: Mortimer House, 37-41 Mortimer Street, London W1T 3JH, UK



Nucleosides, Nucleotides and Nucleic Acids

Publication details, including instructions for authors and subscription information:

<http://www.informaworld.com/smpp/title~content=t713597286>

Polarized Micro Raman Spectroscopic Studies of Nucleic Acid: Local Raman Tensors in Inosine-5'-monophosphoric Acid and the Orientation of Ekyoxanthine Residue in Poly(rI). Poly(rC) Fiber

Koichi Ushizawa^a; Toyotoshi Ueda^a; Masamichi Tsuboi^b

^a Department of Chemistry, Meisei University, Tokyo, Japan ^b Department of Fundamental Science, Iwaki-Meisei University, Iwaki, Fukushima, Japan

To cite this Article Ushizawa, Koichi , Ueda, Toyotoshi and Tsuboi, Masamichi(1996) 'Polarized Micro Raman Spectroscopic Studies of Nucleic Acid: Local Raman Tensors in Inosine-5'-monophosphoric Acid and the Orientation of Ekyoxanthine Residue in Poly(rI). Poly(rC) Fiber', Nucleosides, Nucleotides and Nucleic Acids, 15: 1, 569 — 584

To link to this Article: DOI: 10.1080/07328319608002406

URL: <http://dx.doi.org/10.1080/07328319608002406>

PLEASE SCROLL DOWN FOR ARTICLE

Full terms and conditions of use: <http://www.informaworld.com/terms-and-conditions-of-access.pdf>

This article may be used for research, teaching and private study purposes. Any substantial or systematic reproduction, re-distribution, re-selling, loan or sub-licensing, systematic supply or distribution in any form to anyone is expressly forbidden.

The publisher does not give any warranty express or implied or make any representation that the contents will be complete or accurate or up to date. The accuracy of any instructions, formulae and drug doses should be independently verified with primary sources. The publisher shall not be liable for any loss, actions, claims, proceedings, demand or costs or damages whatsoever or howsoever caused arising directly or indirectly in connection with or arising out of the use of this material.

**POLARIZED MICRO RAMAN
SPECTROSCOPIC STUDIES OF NUCLEIC ACID :
LOCAL RAMAN TENSORS IN INOSINE-5'-
MONOPHOSPHORIC ACID
AND
THE ORIENTATION OF HYPOXANTHINE RESIDUE IN
POLY(rI)·POLY(rC) FIBER[‡]**

Koichi Ushizawa¹, Toyotoshi Ueda^{1*}, and Masamichi Tsuboi²

¹Department of Chemistry, Meisei University, Hodokubo, Hino, Tokyo 191, Japan,

²Department of Fundamental Science, Iwaki-Meisei University, Iwaki, Fukushima 970, Japan

Abstract: The polarized Raman spectra of a single crystal of the barium salt of inosine monophosphoric acid hexahydrate (Ba-IMP·6H₂O) have been observed with 488.0 nm excitation. For each Raman band, the relative intensities of *aa*, *bb*, *cc*, *ab* and *bc* tensor components have been determined. The tensor quotients from the crystal were augmented with measured depolarization ratios in solution. From these experimental data, the shape and orientation of the localized Raman scattering tensor were deduced for each of the normal modes of the hypoxanthine residue, phosphate moiety and ribose portion. The hypoxanthine residue gives a strong Raman band around 1553 cm⁻¹, which shows rather large depolarization ratio, $\rho = 0.32$, in aqueous solution, and shows a great scattering anisotropy in the single crystal of IMP. The shape and orientation of the Raman tensor associated to this 1553 cm⁻¹ vibration have been determined: one of its principal axes (*y*-axis) is directed along the long axis (N1–N7) of the hypoxanthine residue and the relative magnitudes of its components are given as $r_1 = \alpha_{xx}/\alpha_{zz} = -1$, $r_2 = \alpha_{yy}/\alpha_{zz} = 12$. Next, a general relation has been shown between the orientation angles (θ and χ) of such a local Raman tensor in a uniaxial biological fiber and the anisotropy of Raman scattering intensities from the fiber. By the use of this relation, a discussion has been made of the orientation of the hypoxanthine residue in a poly(rI)·poly(rC) duplex fiber.

[‡]This paper is dedicated to Professor Yoshihisa Mizuno on the occasion of his 75th birthday.

INTRODUCTION

This is a part of our series of studies carried out with an attempt to promote a new type of application of Raman spectroscopy to biomolecular research, in which polarized radiations and well-oriented crystals are dealt with. Along this line, single crystals of $d(\text{CGCGCG})_2^1$, ATP^2 , thymine & thymidine³, cytidine & deoxycytidine⁴, uridylyl-(3',5')-adenosine⁵, aspartame⁶ and acetyl-L-tryptophan⁷, and oriented fibers of A- & B-DNA⁸, poly(rA)·poly(rU)⁵, fowl feather barb⁹ and some other biopolymers¹⁰ have so far been subjected to our examinations.

In the classical Raman effect, i.e. when visible laser excitation is employed to excite the Raman spectrum, the intensity of each Raman band is determined by the change of polarizability associated with the corresponding normal mode of molecular vibration. The polarizability derivative tensor (Raman scattering tensor) is defined by the orientation of the principal axes, x , y and z , with respect to the atomic group in the molecule, and by the relative magnitude of the components, α_{xx} , α_{yy} and α_{zz} , of the polarizability derivative with respect to the normal coordinate in question. Once this is established, this would facilitate to determine the orientation of atomic groups (base residue, phosphate moiety and ribose portion) in a given biological system. As data for determining such Raman tensors, polarized Raman spectra of proper single crystals are primarily relevant, and as an auxiliary data, depolarization ratios for relevant molecules oriented randomly in solution are useful.¹¹ In our present work, inosine-monophosphoric acid crystal with a known structure¹² has been subjected to our investigation. Our examination on the depolarization ratios in its solution indicated that the 1553 cm^{-1} band of the hypoxanthine residue has an anisotropic tensor, and that this band must be useful in an orientation study of this residue in a biopolymer. Actually, such a study has subsequently been made of poly(rI)·poly(rC) fiber, and the result was compared with what was found by a previous X-ray diffraction study.¹³

MATERIALS AND EXPERIMENTAL METHODS

Samples for Raman spectroscopy

Purified samples of IMP and poly(rI)·poly(rC) were purchased from YAMASA-SHOYU Co. The IMP crystal was prepared by evaporation from aqueous solution.¹² The poly(rI)·poly(rC) fiber was obtained by sheering viscous solution: i.e. 1 mg of the sample was put on a glass plate and a drop of water was added. The fiber was kept for two days in the air of 92 % relative humidity before it was subjected to the Raman measurement.

The Ba-IMP·6H₂O single crystal was obtained in a plate shape with dimensions of $0.2 \times 1.0 \times 0.4\text{ mm}$. It belongs to an orthorhombic system with the space group of $P2_12_12_1$. Its a -axis is perpendicular to the plane of the plate. The crystallographic b - and c -axes are

in the plane of the plate, with b along the elongated direction.¹² Its size was found to be sufficient for a significant measurement of the scattering intensities I_{aa} , I_{bb} , and I_{cc} corresponding to the aa , bb , and cc components of the crystalline Raman tensor.

Methods of spectroscopic measurements

Raman microscopy of IMP single crystal

First, the Raman spectra were recorded by placing the flat plane (bc -plane) of an IMP single crystal horizontally on the sample stage of a Jasco R-MPS-22 Raman microscope, which was connected to a Jasco NR-1100 Raman spectrophotometer. For exciting Raman scattering, the 488.0 nm beam from an NEC GLG-3300 Ar⁺ laser was used. The beam was sent down through an objective (50×) onto the crystal. The beam was polarized in the front-to-back direction on the sample stage. The crystallographic b -axis was placed parallel to this direction. The backward Raman scattering was collected by the same objective. Then the scattering beam went through a beam splitter, an analyzer and a scrambler into the entrance slit of the spectrophotometer. The analyzer was set so that only the scattered beam polarized along the same direction with the exciting beam can reach the entrance slit. The Raman spectrum observed in this setting with slit width of 5 cm⁻¹ is shown in FIG.1, bb . The excitation laser power was about 50 mW at the laser head and was estimated to be 7 mW on the sample crystal. Next, Raman spectrum for cc setting was recorded, after rotating the flat sample crystal in the horizontal plane by 90°, and by keeping the polarizer and analyzer positions unchanged. Thirdly, the sample crystal was placed with its ab -plane in the horizontal plane on the sample stage. Thus, aa and bb spectra were recorded. The ab spectrum was recorded, after the aa (with the ab -plane of the sample in the horizontal plane) measurement, by rotating the analyzer by 90° and by keeping the a -axis of the sample along the front-to-back direction. Likewise, the bc spectrum was recorded, after the bb (with bc -plane horizontal) measurement, by 90° rotation of the analyzer. In these ab and bc settings, however, the intensities of the bands were all found very weak, and the relative intensities of I_{ab} and I_{bc} were not readily determined. The observed aa , bb , cc , ab and bc spectra are shown in FIG.1. The frequencies and the intensity ratios, I_{aa}/I_{bb} and I_{bb}/I_{cc} , of some prominent Raman bands are listed in TABLE 1.

Depolarization measurements of IMP solution

A Raman spectroscopic measurement was made of an aqueous solution of Ba-IMP, whose concentration was 0.6 M and whose pH was 7.6. At this pH, the phosphate group should have the PO₃²⁻ form. A Jasco NR-1100 spectrophotometer was used with 488.0 nm excitation. A polarizer (analyzer) and an optical scrambler were placed in front of the entrance slit. The Raman scattering intensity $I_{//}$ is for the scattered light polarized

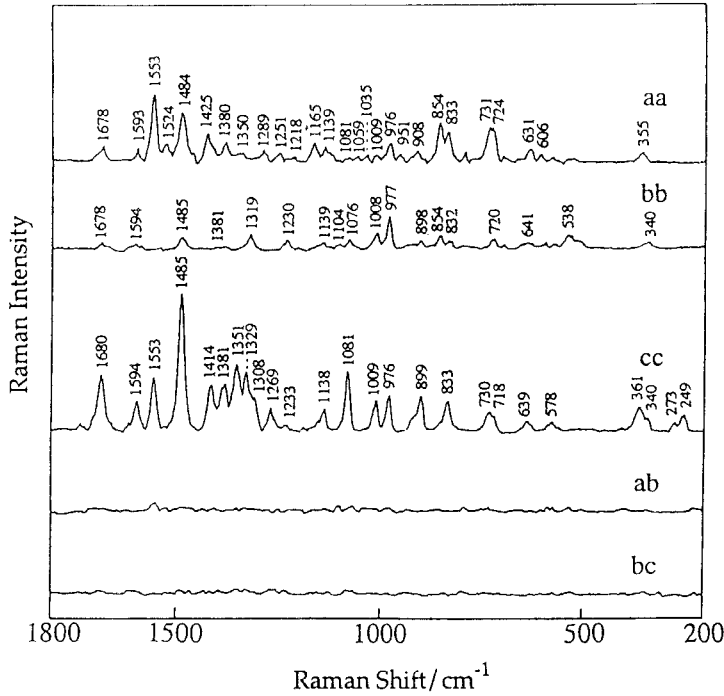


FIG.1. Polarized Raman spectra of a single crystal of Ba-IMP·6H₂O corresponding to five different orientations of the crystallographic axes with respect to the electric vectors of the exciting and scattering radiations. *aa* means, for example, that the electric vector of the exciting beam is placed parallel to the crystallographic *a*-axis, and that the electric vector of the Raman scattering beam is also parallel to the *a*-axis.

TABLE 1. Raman bands of IMP and their possible local Raman tensors

Freq. (cm ⁻¹)	Mode ^a	Obs. <i>I_{aa}</i> / <i>I_{bb}</i>	Obs. <i>I_{bb}</i> / <i>I_{cc}</i>	Obs. depol. ratio	Axis system	Local Raman tensors		Calc. depol. ratio	Calc. <i>I_{aa}</i> / <i>I_{bb}</i>	Calc. <i>I_{bb}</i> / <i>I_{cc}</i>
						<i>r</i> ₁	<i>r</i> ₂			
1678	C=Ostr.	2.09±0.10	0.139±0.006	0.17±0.04	I5	13.4±0.6	4.7±0.3	0.16	2.09	0.139
1594	base ring	2.02±0.10	0.233±0.014	0.10±0.04	I1	2.6±0.3	4.3±0.5	0.08	2.02	0.233
1553	base ring	89±6	0.015±0.010	0.32±0.03	I4	-1.0±0.5	12±3	0.33	93.4	0.020
1485	base ring	3.70±0.20	0.099±0.004	0.13±0.04	I2	4.8±0.2	10.0±0.4	0.12	3.70	0.100
1425	5'-CH ₂ scis.	∞	-----	0.4±0.1	5'-CH ₂	-2	10	0.40	805	0.22
1381	base ring	3.52±0.30	0.084±0.008	0.17±0.06	I2	5.3±0.4	12.9±0.7	0.15	3.52	0.084
976	PO ₃ ²⁻ sym. str.	0.58±0.01	0.955±0.020	<0.01	P3	1.03±0.06	0.76±0.07	0.005	0.581	0.960
899	ribose ring br.	0.37±0.20	0.261±0.040	0.10±0.05	R2	4.8±0.7	2.5±0.6	0.09	0.37	0.263
730	base ring br.	3.25±0.10	0.533±0.013	0.07±0.04	I1	2.3±0.6	1.8±0.3	0.03	3.23	0.533

^a str. = stretching, scis.= scissoring, br. = breathing.

parallel to the polarization direction of the exciting light, and I_{\perp} is for that polarized perpendicular to the polarization direction of the exciting light. The observed depolarization ratio ($\rho' = I_{\perp} / I_{\parallel}$) has been corrected (into ρ) as described in the previous paper.¹¹ The observed spectra are shown in FIG.2, and the wavenumbers and the corrected depolarization ratios (ρ) of some prominent Raman bands are listed in TABLE 1.

Polarized Raman measurement of poly(rI)·poly(rC) fiber

Here, the Raman microscopic measurement was carried out in a similar manner to what was described above for the IMP crystal. In this fiber the molecules are considered to have a uniaxial arrangement. Thus, crystallographic *a*- and *b*-axes are equivalent, both perpendicular to the fiber axis *c*. The observed *bb* and *cc* spectra are shown in FIG.3. As may be seen here, the *cc* arrangement gives practically no Raman bands in the 1800–1200 cm⁻¹ region.

Procedures of analysis

Group theoretical predictions for IMP crystal

The crystal of IMP now in question belongs to the space group $P2_12_12_1$. It contains two IMP molecules in the asymmetric unit and the Bravais unit cell contains eight molecules. Each IMP molecule consists of 34 atoms, and hence the number of optically active, internal normal vibrations is $(3 \times 34 - 6) \times 8 = 768$. The isomorphous point group for this space group is D_2 . Therefore, the optically active 768 normal vibrations are classified into four types: $192A$, $192B_1$, $192B_2$, and $192B_3$ type vibrations. The *A*-type vibrations should appear in the spectra corresponding to the *aa*, *bb*, and *cc* components of the Raman tensor of the crystal; B_1 -type vibrations in the *ab* component; the B_2 -type vibrations in the *ca* component, B_3 -type vibrations in the *bc* component. For the IMP crystal, the Raman bands corresponding to the *ab* and *bc* components are all found to be extremely weak. Hereafter, therefore, we deal with the *A* type vibrational modes only. Information of the local Raman tensors is to be obtained only through the observed I_{aa}/I_{bb} and I_{bb}/I_{cc} intensity ratios.

Derivation of Raman tensors

The Raman tensor is a tensor connecting the electric vector of the exciting radiation and the electric vector of the Raman scattering radiation. In general, it has six components; but when the principal axes (*x*, *y*, *z*) are adopted, it has only three components α_{xx} , α_{yy} , and α_{zz} . Usually, only the relative magnitudes of these three components, defined as

$$r_1 = \alpha_{xx}/\alpha_{zz} \quad \text{and} \quad r_2 = \alpha_{yy}/\alpha_{zz} \quad (1)$$

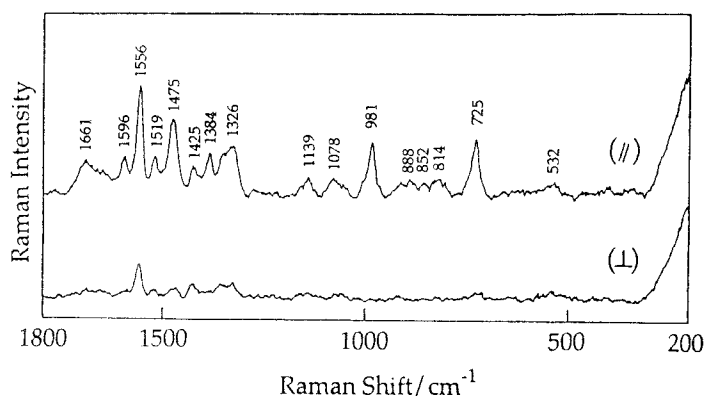


FIG.2. Raman spectra of 0.6 M aqueous solution of Ba-IMP (pH = 7.6) observed in the 90° scattering geometry using 488.0 nm line of the Ar^+ laser. ($//$), the intensity of the Raman scattering beam polarized in the same direction with that of the exciting beam. (\perp), the intensity of the Raman scattering beam polarized in perpendicular direction to that of the exciting beam.

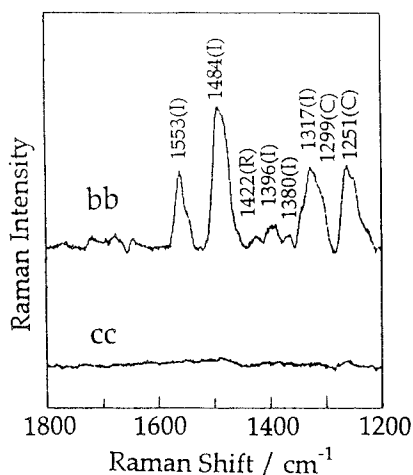


FIG.3. Polarized Raman spectra of oriented fiber of poly(rI)·poly(rC) kept in the air of 92 % relative humidity. *bb*, the electric vectors of exciting and scattering radiations are both perpendicular to the fiber axis *c*. *cc*, the electric vectors of exciting and scattering radiations are both parallel to the fiber axis *c*.

are subjected to our study. Each of such tensors of IMP, some of which are isotropic and some anisotropic, is now to be determined. The Raman intensity ratios, I_{aa}/I_{bb} and I_{bb}/I_{cc} , are related with the local Raman tensors (x, y, z) by the following equations:

$$\frac{I_{aa}}{I_{bb}} = \frac{[\sum (l_x)_i^2 r_1 + \sum (l_y)_i^2 r_2 + \sum (l_z)_i^2]^2}{[\sum (m_x)_i^2 r_1 + \sum (m_y)_i^2 r_2 + \sum (m_z)_i^2]^2} \quad (2)$$

$$\frac{I_{bb}}{I_{cc}} = \frac{[\sum (m_x)_i^2 r_1 + \sum (m_y)_i^2 r_2 + \sum (m_z)_i^2]^2}{[\sum (n_x)_i^2 r_1 + \sum (n_y)_i^2 r_2 + \sum (n_z)_i^2]^2} \quad (3)$$

Here, l_x, m_x, \dots, n_z are the direction cosines; thus, l_x, m_x, n_x are defined as direction cosines of the local x -axis placed in the rectangular abc coordinate system; l_y, m_y, n_y are those for the y -axis, and l_z, m_z, n_z are those for the z -axis. Because the crystal contains two IMP molecules in the asymmetric unit, the summation should be performed for $i = 1$ and 2 . The depolarization ratio, ρ , on the other hand, is defined for molecules oriented randomly in solution, and is given in terms of r_1 and r_2 as^{6,11}

$$\rho = \frac{1.5[(r_1 - r_2)^2 + (r_2 - 1)^2 + (1 - r_1)^2]}{5(r_1 + r_2 + 1)^2 + 2[(r_1 - r_2)^2 + (r_2 - 1)^2 + (1 - r_1)^2]} \quad (4)$$

To reach each Raman tensor of the IMP crystal, we have adopted the procedure described in previous papers^{1,2}. We defined each trial principal axis system by choosing three non-linearly arranged atoms (A, E1, and E2) in an atomic group of the molecule. Thus, the y -axis is defined to be parallel to the line connecting atoms E1 and E2, the x -axis is defined to be perpendicular to the y -axis and involving A, and the z -axis is defined perpendicular to the xy plane. The principal axes selected in this manner for several atomic groups of the IMP molecule are shown in FIG.4. The atoms selected as A, E1 and E2 for each set of principal axes are given in TABLE 2. The intensity ratios, I_{aa}/I_{bb} and I_{bb}/I_{cc} , are now calculated for any trial set of values of r_1 and r_2 by the use of Eqs. (2) and (3). It is practical to calculate contour lines of I_{aa}/I_{bb} and I_{bb}/I_{cc} in the two dimensional coordinate space ($r_1 - r_2$). Such contour maps are shown in FIG.5. The contour map of the depolarization ratio ρ , as calculated by Eq. (4), was given in previous papers.^{6,8,11,14} This r - ρ diagram is useful for selecting sensible choice of the r_1 and r_2 set that is consistent with a given value of ρ . This is to be drawn in the same ($r_1 - r_2$) space as that given for

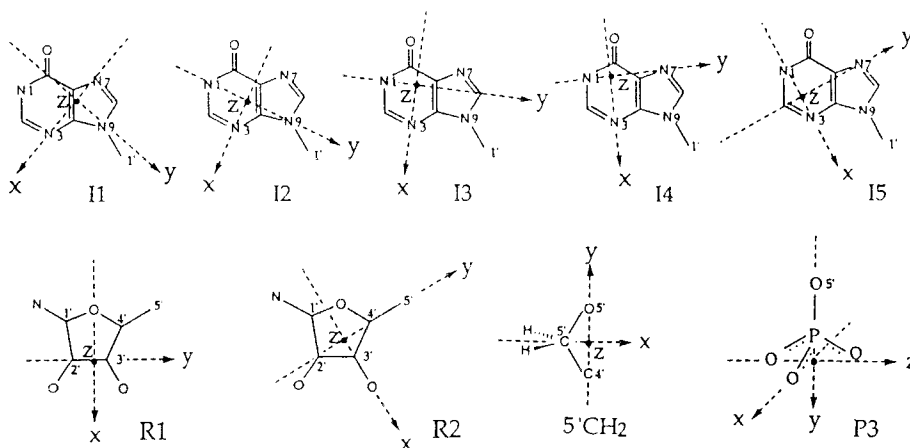


FIG.4. The principal axis systems (x, y, z) of local Raman tensors assumed for some vibrations of the hypoxanthine residue, phosphate moiety and ribose portion. The assumptions were made by selecting three atoms A, E1 and E2 in the vibrating group as described in the text (see TABLE 2).

TABLE 2. Principal axes of the Raman tensors for localized vibrational modes of the IMP molecule.

System ^a	Residue	Atoms used to define axes		
		A	E1	E2
I1	hypoxanthine	N3	C6	N9
I2	hypoxanthine	N3	N1	N9
I3	hypoxanthine	N3	N1	C8
I4	hypoxanthine	N3	N1	N7
I5	hypoxanthine	N3	C2	N7
P3	phosphate	O	P	O5'
R1	ribose	O1'	C2'	C3'
R2	ribose	C3'	C2'	C4'
5'-CH ₂	methylene	C5'	H	H ^b

^a See FIG.4.

^b Coordinates of the hydrogen atoms are not known. For 5'-CH₂, the axes (x, y, z) are defined with A=C5', E1=O5', E2=C4'; and then y and z are interchanged.

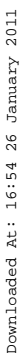


FIG.5. Theoretical I_{aa}/I_{bb} and I_{bb}/I_{cc} values represented in the (r_1, r_2) space for the Ba-IMP-6H₂O single crystal, based upon the atomic coordinates of Nagashima & Iitaka.¹² Each pair of square maps arranged vertically corresponds to a particular one of the principal axis systems given in FIG. 4 (I1 or I2, for example). Each contour line in the map defines the set of coordinates $(r_1$ and $r_2)$, consistent with a particular I_{aa}/I_{bb} or I_{bb}/I_{cc} value indicated on the line.

I_{aa}/I_{bb} and I_{bb}/I_{cc} . From such overlapped maps of I_{aa}/I_{bb} , I_{bb}/I_{cc} and ρ , and by referring to the observed values of I_{aa}/I_{bb} , I_{bb}/I_{cc} and ρ , a suitable set of r_1 and r_2 values must be reached.

RESULTS AND DISCUSSIONS

A preliminary review on the Ba-IMP spectra

The asymmetric unit of the Ba-IMP crystal is composed of two molecules.¹² Both of them have their base planes nearly parallel to the crystallographic *ac*-plane as shown in FIG.6(a). As are seen in FIG.1, the intensities of *aa* and *cc* components for the 1678, 1594, 1553, 1485, 1381 and 730 cm^{-1} Raman bands are all stronger than the corresponding *bb* component. These bands are assignable to the in-plane ring vibrations of the hypoxanthine residue. The depolarization ratios ($\rho = I_{\perp} / I_{\parallel}$) of the Raman bands in aqueous solution corresponding to the 1678, 1594, 1485, 1381 and 730 cm^{-1} Raman band in the crystal are all smaller than 0.2 (FIG.2 and TABLE 1). This fact indicates that each of these Raman tensors must be comparatively isotropic. On the other hand, the depolarization ratio of the 1553 cm^{-1} band is markedly greater (0.32), as is noticeable at a glance of FIG.2. The corresponding Raman tensor must be anisotropic.

For the band at 976 cm^{-1} assigned to the anionic PO_3^{2-} symmetric stretching vibration, the *bb* component is comparable to the *cc* component, and is greater than the *aa* component (FIG.1). In the asymmetric unit of the crystal, there are two PO_3^{2-} groups as shown in FIG.6(b). In the H_2O solution, the 981 cm^{-1} band is assignable to the anionic PO_3^{2-} symmetric stretching vibration. The depolarization ratio of this band is extremely small; its Raman tensor must be quite isotropic.¹¹ The PO_3^{2-} group has a local symmetry of C_{3v} and the Raman tensor of this localized vibration would have pseudo axial symmetry about the C_3 axis.

The band at 899 cm^{-1} is assignable to the ribose ring vibration.¹⁵ In the crystal, the pseudo plane of this five-membered ring is in all the time oriented nearly perpendicular to the *a*-axis as shown in FIG.6(c). As is expected from this orientation, Raman intensity for the *aa* component is weaker than that for the *cc* component (FIG.1). The ρ value of this band (888 cm^{-1}) is around 0.1. This Raman tensor must, therefore, be rather isotropic.

Local Raman tensors in IMP

Hypoxanthine residue

For the 1553 cm^{-1} band of the IMP crystal, we found that, $I_{aa}/I_{bb} = 89 \pm 6$ and $I_{bb}/I_{cc} = 0.015 \pm 0.010$; thus, I_{bb} is very weak (FIG.1). As mentioned above, its depolarization ratio is peculiarly high ($\rho = 0.32 \pm 0.03$) (FIG.2). This suggests that either one of r_1 and r_2

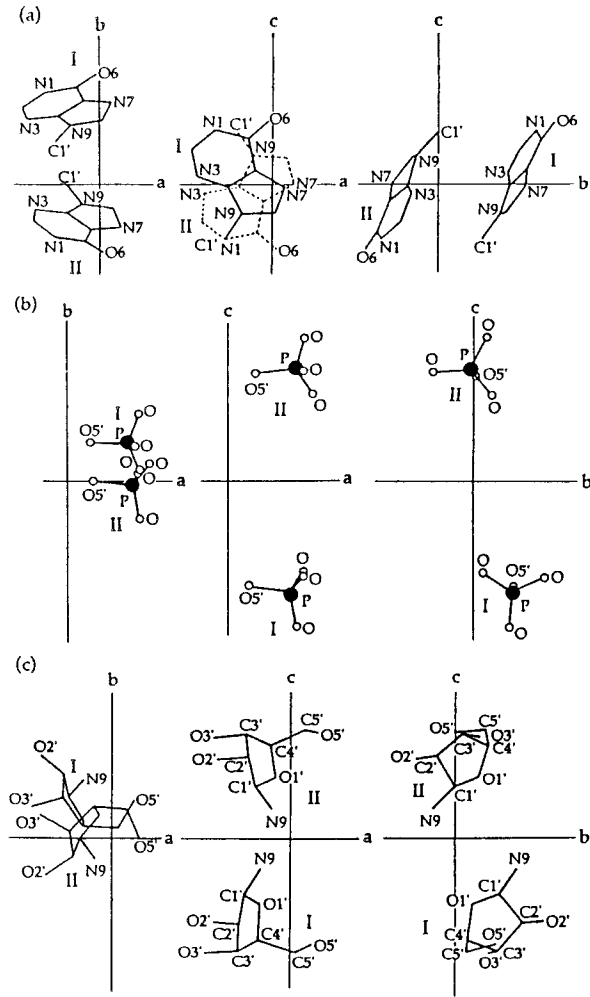


FIG.6. Diagram of the Ba-IMP·6H₂O crystal structure.¹² (a) The orientations of the hypoxanthine residues of the two IMP molecules, I and II in the asymmetric unit of the crystal. (b) The orientations of the two phosphate groups in the asymmetric unit of the crystal. (c) The orientations of the two ribose portions in the asymmetric unit of the crystal.

values is great, while the other is small with different sign.^{1,2,11} By use of the $I_{aa}/I_{bb}-r$, $I_{bb}/I_{cc}-r$ and $\rho-r$ diagrams (FIG.5, see also FIG.1 of ref.8 for example), we found that the set of values $r_1 = -1 \pm 0.5$ and $r_2 = 12 \pm 3$ with the principal axis system of I4 gives the best agreement with the data (FIG.4 and TABLE 1). Such a shape and orientation of this tensor means that, as the amplitude along the normal coordinate of this vibration increases, the molecular polarizability increases greatly along the y -axis, decreases slightly along the x -axis, and increases slightly in the out-of-plane (z -axis) direction. Benevides et al.¹ estimated the Raman tensors of several prominent bands for a $d(\text{CGCGCG})_2$ single crystal, and they obtained a set of values, $r_1 = -1$ and $r_2 = 20-23$, for the 1579 cm^{-1} band of guanine residue. However, they could not fix the principal axis system for this band. This vibration of the guanine residue is probably similar to the 1553 cm^{-1} vibration of the hypoxanthine residue. Therefore, the principal axis system would also be similar to each other in these two purine tensors. In other words the y -axis of the guanine 1579 cm^{-1} tensor is now suggested to be along the long axis of the purine ring.

For the 1485 cm^{-1} vibration of the hypoxanthine residue, the experimental values of $I_{aa}/I_{bb} = 3.70 \pm 0.20$, $I_{bb}/I_{cc} = 0.099 \pm 0.004$ (FIG.1), and $\rho = 0.13 \pm 0.04$ (FIG.2) were obtained. For this data, a set (I2, $r_1 = 4.8 \pm 0.2$ and $r_2 = 10.0 \pm 0.4$) was found to be most preferable (FIGs.4 & 5 and TABLE 1). In the crystal of $d(\text{CGCGCG})_2$, the corresponding guanine vibration is considered to take place at 1486 cm^{-1} , and for its Raman tensor the following estimated values were given: $4 < r_1 < 5$ and $9 < r_2 < 10$.¹ It is interesting that the 1485 cm^{-1} vibration of hypoxanthine and the 1486 cm^{-1} vibration of guanine are found to have nearly equal set of (r_1 , r_2) values. For the guanine 1486 cm^{-1} vibration, the principal axes were not previously given. It has now become probable that G1 axis system defined by Benevides et al.¹, which is similar to our I2 system, would be properly chosen.

The two bands at 730 and 720 cm^{-1} are both assigned to the ring breathing vibrations of the hypoxanthine residue. The appearance of two Raman bands here in the crystal in question is speculated to be caused by a vibrational coupling between the two molecules (I and II) whose base planes are stacked on each other (FIG.6(a)). By estimating integrated intensities over these two bands², we found that $I_{aa}/I_{bb} = 3.25 \pm 0.10$, $I_{bb}/I_{cc} = 0.533 \pm 0.013$ from FIG.1. Since ρ is as small as 0.07 ± 0.04 for this band, the Raman tensor for this mode must be isotropic (FIG.2 and TABLE 1). From a composition of these data, the following tensor is reached: principal axis system II, $r_1 = 2.3 \pm 0.6$ and $r_2 = 1.8 \pm 0.3$ (FIGs.4 & 5 and TABLE 1).

The Raman tensors for some of other vibrations (1678 , 1594 and 1381 cm^{-1}) of hypoxanthine residue, at which we arrive, are also listed in TABLE 1.

Phosphate moiety

For the 976 cm^{-1} band (PO_3^{2-} symmetric stretching vibration), the intensity ratios are found as $I_{aa}/I_{bb} = 0.58 \pm 0.01$ and $I_{bb}/I_{cc} = 0.955 \pm 0.020$ from FIG.1, and the ρ value smaller than 0.01 from FIG.2. The PO_3^{2-} group has a local symmetry of C_{3v} , whose C_3 axis is defined to be y -axis ($\text{O5}'\text{-P}$ line) (FIG.4). Its r_1 and r_2 values are evaluated to be 1.03 ± 0.06 and 0.76 ± 0.07 , respectively. This means that, $\alpha_{xx} \approx \alpha_{zz}$. Thus, the PO_3^{2-} stretching vibration causes a greater polarizability change along the direction perpendicular to the P-O single bond.¹¹ If the bond-polarizability approximation is brought into this 976 cm^{-1} Raman intensity problem, we should assign to the $\text{P}\cdots\text{O}$ bond a $d\alpha/dr$ (polarizability change due to bond-stretching) value 1.32 times as great as that to the P-O single bond.

Ribose portion

The 1425 cm^{-1} band is assigned to the $5'\text{-CH}_2$ scissoring vibration of the ribose residue. In the crystal, this band appears only for the I_{aa} setting and never for I_{bb} nor I_{cc} (FIG.1). The ρ value for this Raman band is 0.4 (FIG.2). Therefore, α_{xx} and α_{yy} should have different signs from each other. Benevides et al.¹ proposed a tensor with $r_1 = -2$ and $r_2 = 10$ for the CH_2 scissoring vibration in the $\text{d}(\text{CGCGCG})_2$ crystal. Thomas et al.³ assigned the same set of values of r_1 , r_2 to the 1420 cm^{-1} band of A- and B-DNA. For our present case, the same set of values is not contradictory with the experimental data. A more detailed and general discussion of the CH_2 scissoring Raman band was made by Tsuboi et al.¹⁰

In the 850–920 cm^{-1} region, a few prominent Raman bands are expected to appear that are caused by some bond stretching vibrations of the five-membered ribose ring. For thymidine, two Raman bands at 899 and 852 cm^{-1} were found to be assignable to such vibrations on the basis of the result of an examination of some ^{13}C isotope effects.¹⁵ The 899 cm^{-1} band of IMP is another candidate to be assigned to such a ribose vibration. For this band, we found that $I_{aa}/I_{bb} = 0.37 \pm 0.20$, $I_{bb}/I_{cc} = 0.261 \pm 0.040$ and $\rho = 0.10 \pm 0.05$. By use of the contour maps in FIG.5, we estimated that $r_1 = 4.8 \pm 0.7$ and $r_2 = 2.5 \pm 0.6$ with axis system R2. Because this is a rather isotropic tensor, this band is probably assignable to the ring breathing vibration of the ribose portion of IMP.

Orientation of hypoxanthine residue in a poly(rI)·poly(rC) fiber

In general, the orientation of a local Raman tensor (x , y , z) in a uniaxial crystal (a , b , c) is given by the two angles, θ and χ , which are defined as shown in FIG.7. Here, θ is the slant angle of z -axis from the fiber axis (c -axis). χ is the angle from $O\text{-}N$ to $O\text{-}y$, where $O\text{-}N$ is the intersection of the ab and xy planes. The Raman intensity ratio I_{cc}/I_{bb} of

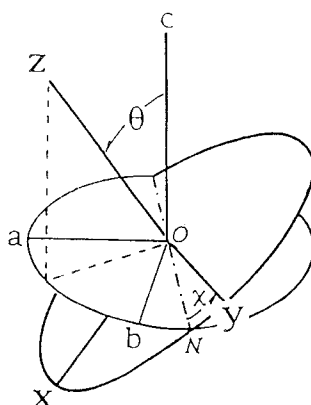


FIG.7. Definition of the angles θ and χ . These angles are for designating the orientation of xyz principal axis system of the Raman tensors (FIG 4) with respect to the crystallographic abc axis system.

a band of this uniaxial crystal (or fiber) is given as a function of such angles (θ & χ) as follows:^{5,6,9}

$$\frac{I_{cc}}{I_{bb}} = \frac{4[\sin^2\theta(r_1\cos^2\chi + r_2\sin^2\chi) + \cos^2\theta]^2}{[\cos^2\theta(r_1\cos^2\chi + r_2\sin^2\chi) + (r_1\sin^2\chi + r_2\cos^2\chi) + \sin^2\theta]^2} \quad (5)$$

If the local tensor is anisotropic, I_{cc}/I_{bb} is expected to be sensitive to the orientation angles (θ & χ). Because we now know that the 1553 cm^{-1} Raman tensor of the hypoxanthine residue is quite anisotropic (I_4 , $r_1 = -1$, $r_2 = 12$), let us examine its orientation in a uniaxial biopolymer fiber. By substituting its r_1 and r_2 values into Eq.(5), the relation of the I_{cc}/I_{bb} value with the orientation angles (θ & χ) is calculated. The result is shown in FIG.8 (left).

For another hypoxanthine band at 1485 cm^{-1} band, whose tensor is less anisotropic (I_2 , $r_1 = 4.8$, $r_2 = 10.0$), the same calculation was made for comparison. The result is shown in FIG.8 (right).

We have made a polarized Raman spectroscopic measurement of an oriented fiber of poly(rl)·poly(rc). The result is shown in FIG.3. As may be seen here, I_{cc}/I_{bb} values are extremely low for almost all the bands observed in the $1800\text{--}1200\text{ cm}^{-1}$ region.

The atomic coordinates of poly(rl)·poly(rc) duplex fiber have been given by Arnott et al.¹³ on the basis of the result of their X-ray diffraction study. The tilt angle θ of the base

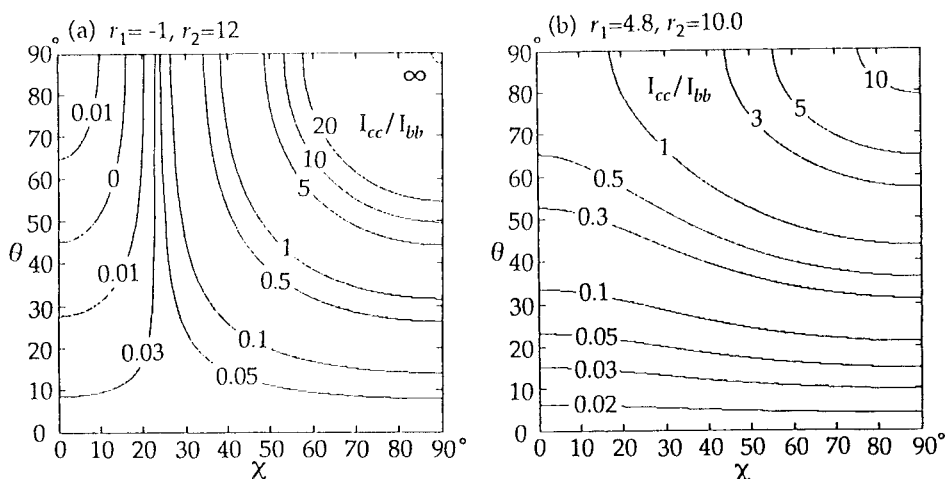


FIG.8. Diagram of I_{cc}/I_{bb} given in the θ - χ space. (a) The Raman intensity ratio I_{cc}/I_{bb} for the 1553 cm^{-1} band expected from a uniaxial orientation (given by θ and χ) of the tensors shown in TABLE 1, third line. (b) Intensity ratio, I_{cc}/I_{bb} for the 1485 cm^{-1} band on the basis of the tensor given in the fourth line of TABLE 1.

plane from the helical axis (c -axis) in the poly(rI)·poly(rC) (A'-RNA) fiber is small and approximately $\pm 11^\circ$.¹³ By the use of their hypoxanthine coordinates, and by assuming the axis system I4, the orientation of the 1553 cm^{-1} tensor is calculated as $\theta = 13^\circ$ and $\chi = 24^\circ$. On the other hand, by assuming the axis system I2, the orientation of the 1485 cm^{-1} tensor is calculated as $\theta = 13^\circ$ and $\chi = 58^\circ$ (FIG.8). The former tensor orientation ($\theta = 13^\circ$, $\chi = 24^\circ$) gives the value of $I_{cc}/I_{bb} = 0.034 \pm 0.004$ according to Eq.(5) (FIG.8(a)). For the latter tensor, ($\theta = 13^\circ$, $\chi = 58^\circ$) set, results in the intensity ratio of 0.038 ± 0.006 (FIG.8(b)). Both of these predicted values of intensity ratios I_{cc}/I_{bb} were in good agreement with what were actually observed. In other words, the poly(rI)·poly(rC) structure derived from the X-ray study has now been supported by our present polarized Raman spectroscopic study.

CONCLUSIONS

By our present polarized Raman spectroscopic study on the single crystal of IMP, a number of local Raman tensors are well characterized. It has been found, for the example, that the Raman tensor for the 1553 cm^{-1} vibration of hypoxanthine residue has the principal axis system I4 and $r_1 = \alpha_{xx}/\alpha_{zz} = -1$ and $r_2 = \alpha_{yy}/\alpha_{zz} = 12$. Such a knowledge of a tensor is useful for presuming the orientation of a functional atomic group in a biological fiber.

ACKNOWLEDGMENTS

We thank Dr. Nobuya Nagashima, Central Research Laboratories, Ajinomoto Co., Inc., for his X-ray diffraction study to fix the crystallographic axes on the IMP crystal used in the present Raman study. Some of the diagrams were drawn by the use of a personal computer by Mr. Tomio Hosaka.

REFERENCES

1. Benevides, J.M., Tsuboi, M., Wang, A.H.-J., and Thomas, G.J., Jr. (1993) *J. Am. Chem. Soc.*, **115**, 5351-5359.
2. Ueda, T., Ushizawa, K., and Tsuboi, M. (1994) *Spectrochim. Acta*, **50A**, 1661-1674.
3. Tsuboi, M., Kumakura, A., Ueda, T., Ushizawa, K., Aida, M., Kaneko, M., and Dupuis, M. (1995) *6th European Conference on the Spectroscopy of Biological Molecules* to be published.
4. Ueda, T., Ushizawa, K., and Tsuboi, M. (1995) *J. Mol. Struct.*, in submission.
5. Tsuboi, M., Ueda, T., Ushizawa, K., and Nagashima, N. (1995) *J. Raman Spectrosc.*, in press.
6. Tsuboi, M., Ikeda, T., and Ueda, T. (1991) *J. Raman Spectrosc.*, **22**, 619-626.
7. Tsuboi, M., Ueda, T., Ushizawa, K., Ezaki, Y., Overman, S.A., and Thomas, G.J., Jr. (1995) *J. Mol. Struct.*, in submission.
8. Thomas, G.J., Jr., Benevides, J.M., Overman, S.A., Ueda, T., Ushizawa, K., Saitoh, M., and Tsuboi, M. (1995) *Biophys. J.*, **68**, 1073-1088.
9. Tsuboi, M., Kaneuchi, F., Ikeda, T., and Akahane, K. (1991) *Can. J. Chem.*, **69**, 1752-1757.
10. Tsuboi, M., Ueda, T., and Ushizawa, K. (1995) *J. Mol. Struct.*, in press.
11. Ueda, T., Ushizawa, K., and Tsuboi, M. (1993) *Biopolymers*, **33**, 1791-1802.
12. Nagashima, N. and Iitaka, Y. (1968) *Acta Crystallogr., Sect. B*, **24**, 1136-1138.
13. Arnott, S., Hukins, D.W.L., and Dover, S.D. (1972) *Biochem. Biophys. Res. Commun.*, **48**, 1392-1399.
14. Thomas, G.J., Jr. and Tsuboi, M. (1993) *Adv. Biophys. Chem.*, **3**, 1-70.
15. Tsuboi, M., Ueda, T., Ushizawa, K., Sasatake, Y., Ono, A., Kainosho, M., and Ishido, Y. (1994) *Bull. Chem. Soc. Jpn.*, **67**, 1483-1484.